Investigation of the photoinduced magnetization of Copper octacyanomolybdates nanoparticles by X-ray Magnetic Circular Dichroism

Sophie Brossard[1], *Florence Volatron*[2], *Laurent Lisnard*[2], *Marie-Anne Arrio*[1*], *Laure Catala*[2], *Corine Mathonière*[3], *Talal Mallah*[2], *Christophe Cartier dit Moulin*[4], *Andrei Rogalev*[5], *Fabrice Whilem*[5], *Alevtina Smekhova*[5], *and Philippe Sainctavit*[1]

[1] Institut de Minéralogie et de Physique des Milieux Condensés, CNRS UMR 7590, Université Pierre et Marie Curie, 4 place Jussieu, Case 115, 75252 Paris cedex 05, France; [2] Institut de Chimie Moléculaire et des Matériaux d'Orsay, Université de Paris 11 Paris-Sud, Bât. 420, 15 rue Georges Clemenceau, 91405 Orsay Cedex, France; [3] CNRS, Université de Bordeaux, ICMCB, 87 av. Du Dr A; Schweitzer, 33608 Pessac Cedex, France; [4] Institut Parisien de Chimie Moléculaire, CNRS UMR 7201, Université Pierre et Marie Curie, 4 place Jussieu, 75252 Paris Cedex 05, [5] European Synchrotron Radiation Facility, 6 rue Jules Horowitz, BP220, 38043 Grenoble Cedex, France.

*Corresponding author : Marie-Anne.Arrio@upmc.fr

Abstract:

Through an extensive set of SQUID magnetic measurements, X-ray absorption spectroscopy and X-ray magnetic circular dichroism, we have determined the nature of the metastable photomagnetic phase in the cyano-bridged 3D network $Cs_2Cu_7[Mo(CN)_8]_4$. The photomagnetic effect is induced by the photoconversion of Mo(IV) ions in Low Spin (LS) configuration (S=0) into Mo(IV) ions in High Spin (HS) configurations (S=1). The magnetic and spectroscopic measurements fully support the LS to HS conversion whereas the previously invoked charge transfer mechanism Mo(IV)+Cu(II) => Mo(V)+Cu(I) can be completely ruled out.

I - Introduction

Bistable magnetic coordination networks that may be tuned by various stimuli (magnetic field, light, pressure, temperature) have been the subject of intense research over the past decades.[1-6] Nanoparticles made of such networks are interesting since this bistability may be controlled at the level of a nano-object. Amongst the chemical compounds that can be used to form such particles, the family of cyanide-bridged coordination networks were found to be of particular interest.[7-16] Indeed, such materials are known to exhibit interesting properties such as ferromagnetism below Curie temperatures that can reach room temperature[2,3,17], spin crossover[4], and particularly photomagnetism[1]: upon irradiation and absorption of photons, changes in the electron configuration of the metallic ions of the structure lead to changes in the magnetic properties. [18,19]

The first compound in which photoinduced magnetization was observed was the Prussian Blue Analogue (PBA) $K_{0.2}Co_{1.4}$- $[Fe(CN)_6]\cdot 6.9H_2O$ in which Co and Fe atoms are linked by cyanides: the fcc network consists in Fe^{II} (S = 0) – CN – Co^{III} (S = 0) pairs yielding a diamagnetic material [5,18-24]. As firstly observed by Shirom *et al*. [25] in solution and in glasses, the $Fe(CN)_6^{4-}$ ions can be excited by irradiation at the bottom of the intervalence band wavelength (λ = 313 nm). For the PBA compounds, upon illumination with visible light, an electron transfer occurs from the iron ions to the cobalt ions, resulting in a metastable state formed by Fe^{III} (S = 1/2) and Co^{II} (S = 3/2) ions with a ferrimagnetic arrangement through the cyanide bridges, which relaxes to the stable

state at temperature up to 120 K depending on the nature and amount of the inserted alkali [5,18-24]. Study of XANES (X-ray Absorption Near Edge Spectroscopy) spectra of the compounds at $L_{2,3}$ and K edges of Fe and Co ions showed energy shifts of the characteristics peaks and intensity modifications, providing support to the hypothesis of the electron transfer [22,24], while the recording of XMCD (X-ray Magnetic Circular Dichroism) signals at the Co K and Fe K edges allowed the characterisation of the spin configuration and spin arrangement in the system [26]. Moreover such effect was found to be reversible by thermal treatment of the compound [18,19], notably XANES spectra before irradiation and after thermal relaxation were comparable [22].

Another class of photomagnetic networks can be synthesized with octacyanomolybdates units as building blocks [18,23,27]. Shirom *et al.* [28] observed the possibility of exciting through laser irradiation $Mo^{IV}(CN)_8^{4-}$ ions in solution or in glasses, then Hennig *et al.* [29,30] showed that associating the $[Mo^{IV}(CN)_8]^{4-}$ ions with Cu^{II} ions led to the formation of donor/acceptor pairs. Following these observations, octacyanomolybdate compounds $Mo(CN)_8(CuL)_x$ (x>1) were developed, in which the photomagnetic behaviour was explained by the following mechanism: the ion $[Mo^{IV}(CN)_8]^{4-}$ become oxidised, upon irradiation by visible light, into $[Mo^{V}(CN)_8]^{3-}$ [18,27,30-34]. While Mo^{IV} (Low Spin d^2) has a spin S = 0, Mo^{V} (d^1) has a spin of S = 1/2. Coupling of the molybdenum ion with Cu ions, through cyanide bridges, creates a system in which the electron transfer would transform Cu^{II} (d^9, S = 1/2) into Cu^{I} (d^{10}, S = 0), and thanks to the ferromagnetic exchange interaction between the central Mo^{V} ion and the remaining Cu^{II} ion, one would observe the magnetic behaviour of a magnetically coupled system. One major implication of the charge transfer mechanism is that the magnetic moment at saturation of one formula unit should remain constant since the oxidation of one Mo^{IV} (S=0) ion into a Mo^{V} (S=1/2) ion is accompanied by the reduction of one Cu^{II} (S=1/2) into Cu^{I} (S=0) ion. Only the shape of the magnetization curve should be modified yielding a steeper increase at low fields due to ferromagnetic interactions. [35-37]

Very recently some of us suggested that photomagnetism in molecules derived from octacyanomolybdates would not result from a charge transfer mechanism[38]. Following the idea of tailoring magnetic properties as a function of size,[39,40] the authors investigated the photomagnetic molecule: $[Mo(CN)_6(CN\text{-}CuL'_2)_2]$ (L' = *N, N'* dimethyl ethylene diamine). They used XANES (X-ray Absorption Near Edge Spectroscopy) and XMCD (X-ray Magnetic Circular Dichroism) at

Mo $L_{2,3}$ edges in order to evaluate the orbit and spin magnetic moment of molybdenum ions.[38] XMCD measurements on photomagnetic compounds track the possible changes induced by photoconversion [41,42] and Arrio *et al*. showed that after X-ray induced photoconversion the Mo ions were High Spin Mo^{IV} (S=1) and not Mo^{V} ions. Consequently it was proposed that instead of a charge transfer, the x-ray induced photoconversion caused a spin conversion between low spin Mo^{IV} ion (S=0) and high spin Mo^{IV} ion (S=1). It should be noted that a recent theoretical study supports this experimental finding with DFT calculations[43].

The present study intends to apply a similar methodology to an extended network of octacyanomolybdate, $Cs_{0.5}Cu_{1.75}[Mo(CN)_8]$ that has been previously synthesized and studied by Hozumi *et al*. in a film prepared by electrochemistry. Hozumi *et al*. [44] observed a larger coercive field (H_c = 350 G) than the one found in the parent $Cu_2[Mo(CN)_8]$ compound (H_c = 7 G) [34,36,45] and higher Curie temperature (23 K instead of 17 K [34,36,45]) that they related to the Cs^+ cations that would induce a double-layered structure. They attributed the photoconversion to a charge transfer mechanism. Moreover, by comparing the Infra Red (IR), Electron Spin Resonance (ESR) spectra, and X-ray Diffraction (XRD) patterns before laser irradiation, after irradiation and after relaxation at room temperature, they concluded that the photomagnetic changes were fully reversible. Ma *et al*. [32] performed XANES on the same compound at the Cu K edge and interpreted the modification of the Cu K-edge under illumination as a Cu^{II} to Cu^{I} reduction. Their interpretation was in line with the charge transfer model upon irradiation. However, since the reversibility of the Cu K-edge signal was not investigated and no reports were made regarding the Mo $L_{2,3}$ edges, the X-ray damages can not be ruled out based on their results. In the present experiment, we have investigated nanoparticles of $[Cs_{0.5}Cu_{1.75}[Mo(CN)_8]_{1.1}]^{0.4-}$ cores surrounded by molecules of DODA where DODA stands for dimethyldioctadecyl-ammonium. Photomagnetism is induced by a 405 nm laser with no X-ray induced photomagnetism and great care is taken to limit the X-ray induced damages. The size of the nanoparticles (i.e. $[Cs_{0.5}Cu_{1.75}[Mo(CN)_8]_{1.1}]^{0.4-}$ cores) is 17 nm ± 3 nm and was chosen so that it is small compared to the penetration depth of the x-rays, thus insuring that the nanoparticles are fully probed by XAS. For the first time in these Cu-Mo photomagnetic compounds, both Mo $L_{2,3}$ edges and Cu K edge have been investigated in the same time. This gives us a more complete description of the photo-induced mechanism than the reported studies performed on similar systems and allows to

clearly identify the presence of HS Mo(IV) in the photomagnetic phase with no need for the charge transfer mechanism.

II - Results

Synthesis and characterization of the nanoparticules

The synthetic procedure and full characterization of the particles may be found in the work published by Volatron *et al.* [46,47] Notably, the DODA organic cations were used to form a shell around the $[Cs_{0.5}Cu_{1.75}[Mo(CN)_8]_{1.1}]^{0.4-}$ charged nanoparticles and facilitate their precipitation from the synthetic solution. In the following, the compound is labelled CsCuMo and the term formula unit (f.u.) refers to a Cs:Cu:$[Mo(CN)_8]$ stoichiometry of 0.5:1.75:1.1.

The magnetic properties of the particles were firstly investigated using a SQUID (Superconducting Quantum Interference Device) MPMS-5S in static mode. Details on the experimental protocol may again be found in the work from Volatron *et al.* [46,47]. Irradiation of the particles was carried on inside the SQUID cavity with an Ar^+-Kr^+ laser (λ = 488 nm, P = 3 $mW.cm^{-2}$) coupled to an optical fibre. SQUID measurements were then made before, and after a 22 hours laser irradiation (see in S.I. Fig. S1a) for various temperatures and magnetic fields. The obtained curves for the magnetic susceptibility χ and the magnetization M are presented in Fig.1.

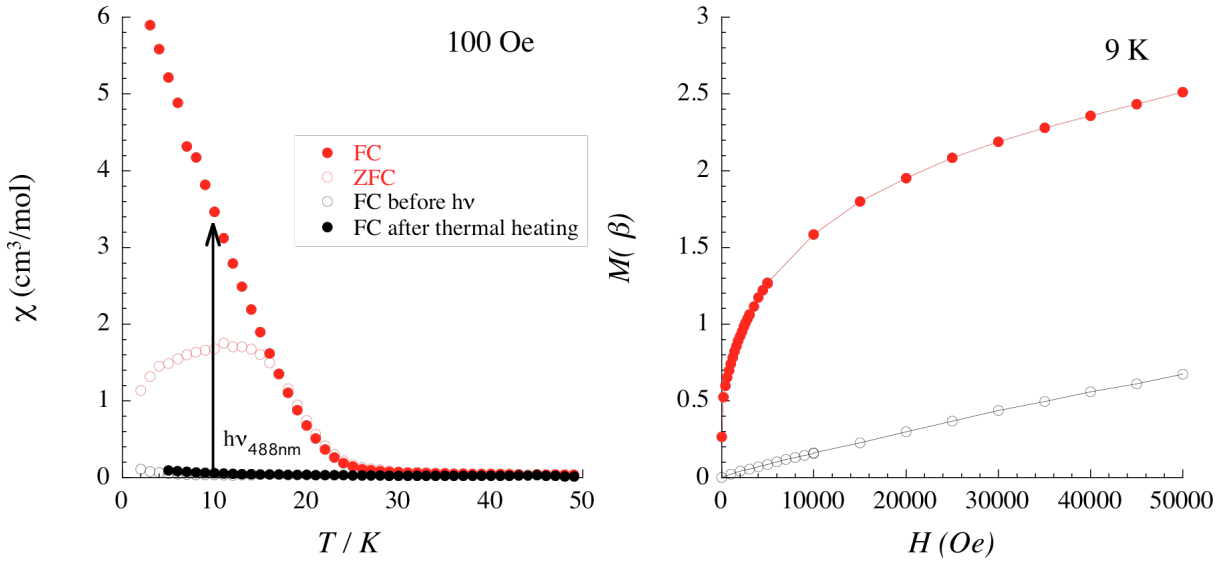

Fig 1. Magnetic measurements before (open dots) and after (full dots) illumination by a 488 nm laser per formula unit (a) χ as a function of Temperature and measured at 100 Oe ; (b) Magnetization in Bohr Magneton, as a function of the external magnetic field and measured at 9 K. [46,47]

As can be seen on Fig.1, before irradiation, the magnetic susceptibility χ and the magnetization M measured at 9 K are typical of a paramagnet with the expected magnetic response of 1.75 Cu^{II} ions, the Low Spin Mo^{IV} ions being diamagnetic [38,46,47]. The magnetization curve displayed in Fig.1b, before illumination, is consistent with the Brillouin curve calculated for 1.75 Cu^{II} ions. Irradiating the compound with a 488 nm laser significantly increases the susceptibility and the magnetization at low temperature (Fig.1a and Fig.1b). After irradiation, the zero-field cooled and field-cooled susceptibilities present a divergence below 20 K (Fig.1a) in agreement with the appearance of a hysteresis loop in the magnetization curve at 2 K with a coercive field around 800 Oe (see in S.I. Fig.S1.b). These data confirm the magnet-like behaviour of the nanoparticles. The magnetization when measured at 2 K tends to saturate at a value close to 3.1 Nβ. When the material is heated at 200 K, the initial susceptibility and the magnetization (before irradiation) are fully recovered (Fig.1a). These data attest the photomagnetic properties of the particles: before irradiation they show a paramagnetic behaviour while after irradiation they are clearly ferromagnetic. These photomagnetic observations are in lines with the ones made on other copper octacyanomolybdate compounds [31,34,48].

XANES and XMCD measurements

The experiments have been performed on the ID12 beamline of the ESRF synchrotron (Grenoble, France) [49]. The flux of circularly polarized photons delivered by the EMPHU undulator is monochromatized by a Si(111) two-crystal monochromator. The circular polarization rate before monochromatization (97%) drops to 12% at the Mo L_3 edge, 4% at the Mo L_2 edge and 70% at the Cu K-edge after monochromatization [50]. The sample is magnetized by a superconducting coil delivering +/- 6 T and cooled down to 9 K. The incoming photon flux is measured by monitoring the fluorescence of a 4 μm thick Ti foil at the Cu K edge and a thin Kapton foil at the Mo $L_{2,3}$

edges. The absorption is recorded in Total Fluorescence Yield (TFY) by a silicon diode. More instrumental information can be found in Ref.[38]. The XMCD signal has been measured by reversing both the photon helicities and the direction of the magnetic induction and obtained by the appropriate averaging of the various cross sections.

The synthesized powder was here pressed in a pellet that was then glued to the copper head of the sample holder with Apiezon grease in order to insure optimal thermal contact. Illumination was carried out with a laser at λ = 405 nm for 7 hours (10 mW/cm^2) (Ref. SHARP Blue Violet laser diode GH04020B2A mounted into a Thorlabs power supply with Thorlabs thermal regulation). The actual photon flux on the sample mounted into the Variable Temperature Insert of ID12 cryomagnet is much less than 10 mW/cm^2 because of geometrical factors and laser divergence. Previous work by Arrio *et al*. showed that irradiation by X-rays during such XAS experiments also induced a magnetic conversion [38], consequently the effects of both Violet and X-ray irradiations were studied and will be discussed.

The XAS spectra were normalized with the following protocol: once the cross-section before the edge is set to 0 by subtraction, the edge jump in the continuum spectral region is set from 0 to 2 for the Mo L_3 edge (ΔL_3=2), from 2 to 3 for the Mo L_2 edge (ΔL_2=1), and 0 to 1 for Cu K edge (see S.I for more details). This allows, for the Mo $L_{2,3}$ edges, to account for the 2/3 statistic branching ratio of the continuum states. Indeed with the spin-orbit coupling, the 2p core level is split into two states: $j = \ell + s = 3/2$ (L_3 edge, 4-fold degeneracy) and $j = \ell - s = ½$ (L_2 edge, 2-fold degeneracy), leading to a $\Delta L_3/(\Delta L_2 + \Delta L_3)$ ratio of 2/3.

The XMCD signal is calculated by doing the difference between the XAS spectra, for a given energy, with right and left circularly polarized x-rays. The specimen magnetization is parallel to the photons wave vector, and in the electric dipole approximation, reversing the photon helicity is equivalent to reversing the magnetic induction. Spectra are recorded in a fixed magnetic field (either + 6 T or - 6 T) and the circular polarization is flipped at each energy point. If we note $\sigma^{\downarrow\uparrow}$ and $\sigma^{\downarrow\downarrow}$ the absorption cross sections with right polarized circular x-rays and for a magnetic field parallel and antiparallel to the photons propagation vector, and $\sigma^{\uparrow\uparrow}$ and $\sigma^{\uparrow\downarrow}$ with left polarized x-rays, then the XMCD signal can be defined as $\sigma_{XMCD} = (\sigma^{\downarrow\uparrow} + \sigma^{\uparrow\downarrow})/2 - (\sigma^{\downarrow\downarrow} + \sigma^{\uparrow\uparrow})/2$. Such sign

convention means that for a 4d transition metal like Mo, a magnetic moment parallel to the applied magnetic field results in a negative value for σ_{XMCD} at the Mo L_3 edge. For sake of comparison the XMCD spectra presented here have been renormalized for a polarization rate equal to 100% and self-absorption corrections due to TFY mode have also been applied. Such corrected spectra allow the calculation of the orbit and spin magnetic moments of the Mo 4d shell, by application of the magneto-optic sum rules, as developed by Thole *et al.* and Carra *et al*. [41,42,51].

The experimental protocol is set as follow. The specimen is cooled down to 9 K and XAS spectra are measured at both Mo $L_{2,3}$ edges and Cu K edge. Laser illumination is then carried out for 7 hours at 405 nm, and one then records Mo $L_{2,3}$ edges and Cu K edge at 9 K. Since the spot size of the laser is much larger than the sample, the whole sample is illuminated. Then around 40 spectra are recorded at Mo $L_{2,3}$ edges for the XMCD measurements. Finally, the temperature of the specimen is raised to 300 K, we wait for temperature stabilization and we measure spectra at Mo $L_{2,3}$ edges and Cu K edge. In order to study the reversibility of the photomagnetic effect, the 300 K spectra are recorded at a location on the specimen that has been laser illuminated but where no x-ray spectra have been measured.

Evolution of the isotropic absorption spectra at the Mo $L_{2,3}$, edges and Cu K edge

Figure 2 display the isotropic absorption spectra measured at the Mo L_3 edge before laser illumination (T = 9 K), after laser illumination (T = 9 K), and after thermally induced relaxation (T = 300K). When comparing the spectra before and after illumination, the apparition of peak A can be noted, whereas a decrease in intensity occurs for peak D. With thermally induced relaxation (T = 300 K), one can note that the changes induced by the illumination are mostly reversible with a small non-reversible contribution. Relaxation is accompanied by a reduction of peak A with a residual contribution and shoulder D becomes a well-defined maximum. Nevertheless the spectrum after relaxation does not completely match the initial spectrum. Such a partial irreversibility has already been observed by Herrera *et al.* [27] and cannot be attributed to x-ray damages since the samples saw only a very reduced x-ray flux. Then shoulder B at 2522 eV mainly corresponds to laser induced damages since x-ray damages have also been minimized in

the present experimental protocol. Similar spectra have been measured at the Mo L_2 edge (see Figure S3 in S.I.) and the evolution of the various peaks is parallel to the one just described for the Mo L_3 edge. The shape of the present XAS signals are very similar to the ones previously measured by some of us in the recent study on a related photomagnetic molecule (See SI Fig S4) [38].

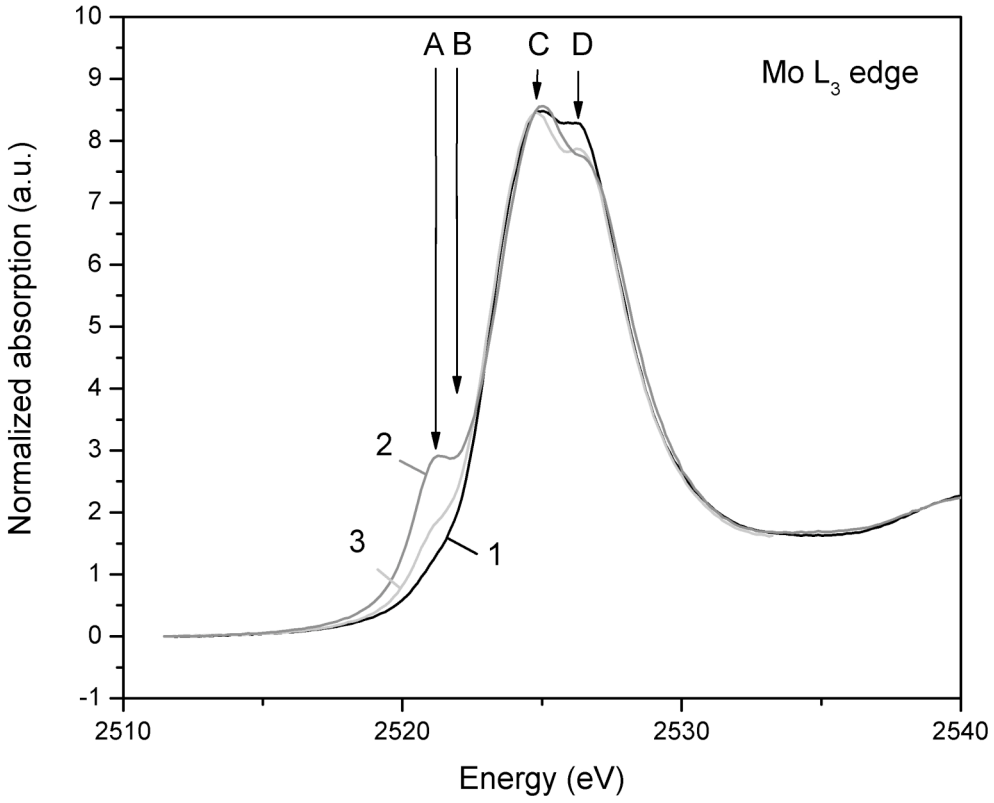

Figure 2. Absorption spectra at the Mo L_3 edge : (**1**) before illumination (T = 9 K); (**2**) after illumination (T = 9 K); (**3**) after relaxation at room temperature (T = 300 K).

Figure 3 displays the different isotropic absorption spectra measured at the Cu K edge before laser illumination (T = 9 K), after laser illumination (T = 9 K), and after thermally induced relaxation (T = 300 K). Peak A at 8987.6 and peak B at 9001.5 eV have been reported in Fig.3. With laser illumination peak A increases and peak B decreases. The variations of intensity for

peaks A and B are very small: it is around 2% of the atomic absorption for peak A and around 5% for peak B. The spectrum recorded at 300 K after thermal relaxation clearly indicates that there is no observable reversibility: the spectrum at 300 K is very much similar to the one measured at T= 9 K after laser illumination.

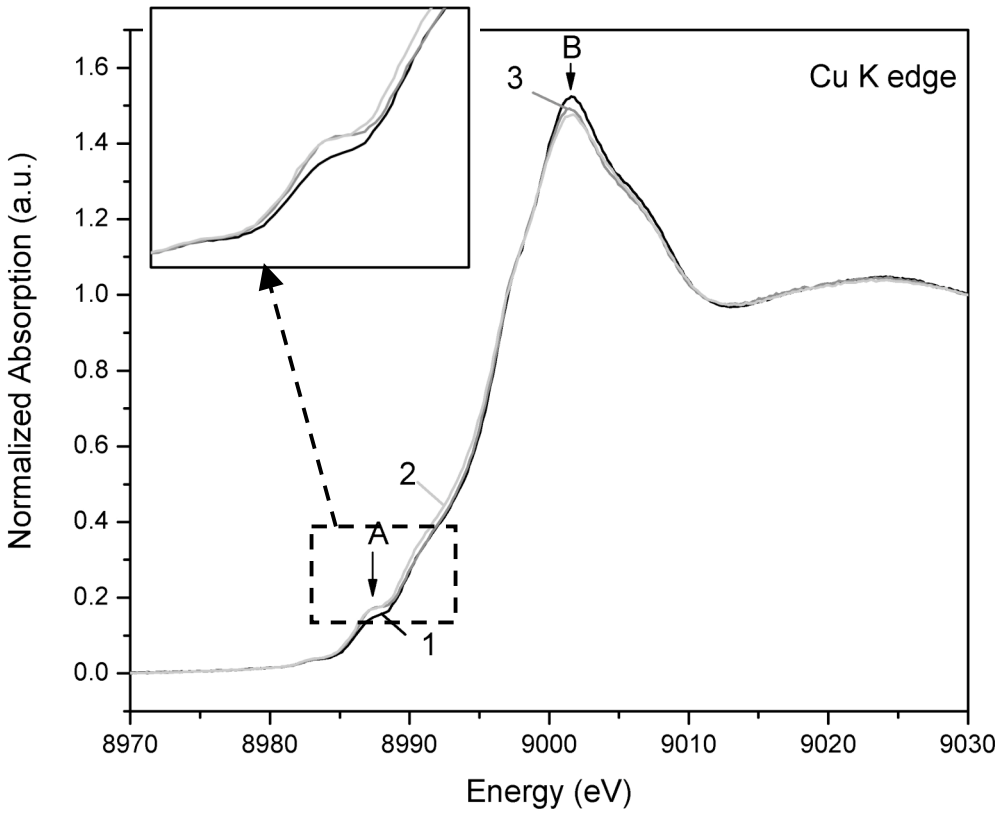

Figure 3. Absorption spectra at the Cu K edge (**1**) before laser illumination (T = 9 K), (**2**) after laser illumination (T = 9 K) and (**3**) after thermally induced relaxation (T = 300 K). The inset displays a zoom on the pre-edge region.

XMCD measurements

Figure 4 reports the isotropic XAS spectra and the XMCD signal measured after laser illumination at the Mo $L_{2,3}$ egdes. Before laser illumination, the XMCD signals were nil, as expected for a diamagnetic ion. After laser illumination, a clear XMCD signal appears at the energy of feature A in Fig.2. The shape of the present XMCD signal is very similar to the one previously measured on a related photomagnetic molecule.[38]

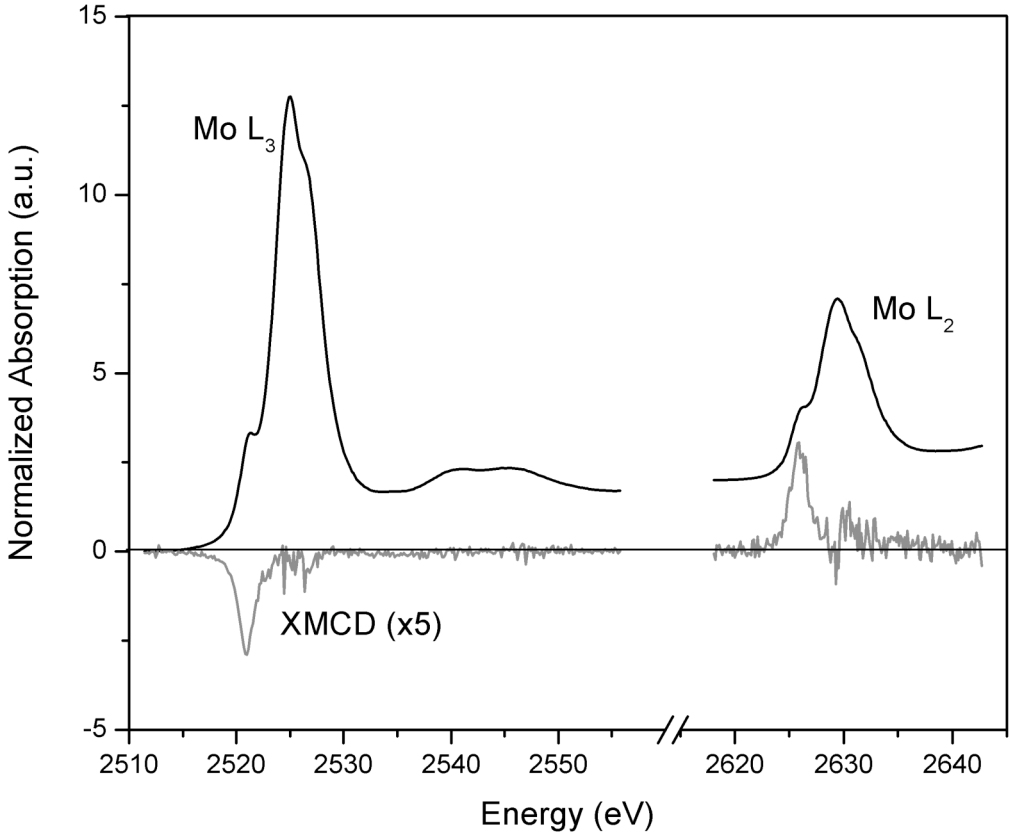

Figure 4. Isotropic XAS spectra and XMCD signals at the Mo $L_{2,3}$ edges recorded at T=9K and H = ± 6T. The XMCD signals have been renormalized to 100% circularly polarized x-rays and multiplied by a factor of 5.

The integration of these signals and the application of the sum rules developed by Thole *et al.* [51] gave the following results for the spin and orbit magnetic moments of Mo. In the hypothesis of Mo^{IV} HS (i.e. n_h, the number of 4d holes is equal to 8), one gets an orbit magnetic moment M_L =

$-\mu_B\langle L_z\rangle = -0.02 \pm 0.005\ \mu_B$ and a spin magnetic moment $M_s = -g\mu_B\langle S_z\rangle = +0.44 \pm 0.05\ \mu_B$, which corresponds to a total magnetic moment $M = M_L + M_S = 0.42 \pm 0.06\ \mu_B$. In the hypothesis of Mo^V ($n_h = 9$), one gets an orbit magnetic moment $M_L = -\mu_B\langle L_z\rangle = -0.02 \pm 0.005\ \mu_B$ and a spin magnetic moment $M_s = -\mu_B\langle S_z\rangle = +0.50 \pm 0.05\ \mu_B$, which corresponds to $M = M_L + M_S = 0.48 \pm 0.06\ \mu_B$.

III – Discussion

Since the discovery of the photomagnetic effect in copper octacyanomolybdates, the photo-induced magnetism was attributed to a charge transfer between a Low Spin Mo(IV) ion and a divalent copper ion and the scheme was said to be Mo(IV) + Cu(II) => Mo(V) + Cu(I). This mechanism was in agreement with the presence of a Metal-Metal Charge Transfer band in the optical spectrum. Recently Arrio *et al*. [38] suggested that this picture might be not so simple. In the present discussion, we show that the charge transfer hypothesis does not hold but that both SQUID measurements and XMCD signals can be quantitatively interpreted if the photo-induced magnetism results from a spin conversion between a Low Spin Mo(IV) ion and a High Spin Mo(IV) ion.

Indeed the SQUID measurements in Fig.1b clearly indicate that the magnetization per formula unit follows the expected Brillouin curve for independent S=1/2 copper ions before laser illumination. Such Brillouin curve saturates at 1.75 Bohr magnetons. After photoconversion one observes a large increase of the magnetization that exceeds the magnetization at saturation before photoconversion. This is in contradiction with the Mo to Cu charge transfer for the photoconversion for which the same saturation values are expected before and after the charge transfer. On the contrary, the hypothesis of the LS (S=0) to HS (S=1) conversion for all Mo ions would give a magnetization at saturation around 3.95 Bohr magneton per formula unit which is compatible with the SQUID measurements (full dots of Fig.1b and Fig.S1b). At this point, the charge transfer hypothesis does not hold at all and this is also confirmed by the following analysis of the x-ray spectroscopic measurements.

From the examination of Fig.2 for Mo $L_{2,3}$ edges, one can see that peak A is the feature associated to the photoconversion. Following the intensity of peak A, one sees that reversibility is almost complete but some partial damage is observed. Since the photoexcitation is mainly

induced by the 405 nm laser illumination due to a very small flux used for x-rays, the difference between spectra **1** and **3** is likely to come from damages induced by the laser. Then we confirm that Mo ions are involved in the photoconversion process as previously determined by Herrera *et al*. [27] and Arrio *et al*. [38]. By comparison of peak A intensity in Fig. 3 with the similar feature from Refs. Herrera *et al.* and Arrio *et al.* [27,38], one can estimate that the photoconversion rate in the present study is in between 30 % and 40 % (See in SI fig SI4). In other words, around 35% ± 5% of the molybdenum ions have been phototransformed and around 65 % ± 5 % of the Mo ions remained in the Mo(IV) Low Spin configuration.

From the analysis of the XMCD spectra we have determined that the average Mo magnetic moment was $0.0525.n_h$ Bohr magneton ($M_{Spin} \approx 0.055.n_h\ \mu_B$ and $M_{Orbit} \approx -0.0025.n_h\ \mu_B$) where n_h is the number of 4d holes (n_h=8 for Mo(IV) ion and n_h=9 for Mo(V) ion). In Fig.4, we have plotted the theoretical magnetization of the Mo ion for an hypothetical High Spin Mo(IV) ions in a Mo(IV)-$Cu(II)_{1.75}$ molecular entity (curve **a**) and for an hypothetical Mo(V) ion in a Mo(V)-Cu(I)-$Cu(II)_{0.75}$ molecular entity (curve **b**) considering a photoconversion yield of 35% ± 5%. The shadowed square in Fig.4 is the measured XMCD magnetization in the case of Mo(IV) (n_h=8) and the shadowed cross is for the case of Mo(V) (n_h=9). From Fig.4, it is clear that the hypothesis of HS Mo(IV) fits well with the experimental data: the shadowed square is sitting within the errors bars of curve **a**. On the contrary, the hypothesis of Mo(V) gives a too small calculated magnetization to explain the experimental value since the shadowed cross is well above the curve **b**. Then the photo-induced formation of Mo(V) is not compatible with the experimental data.

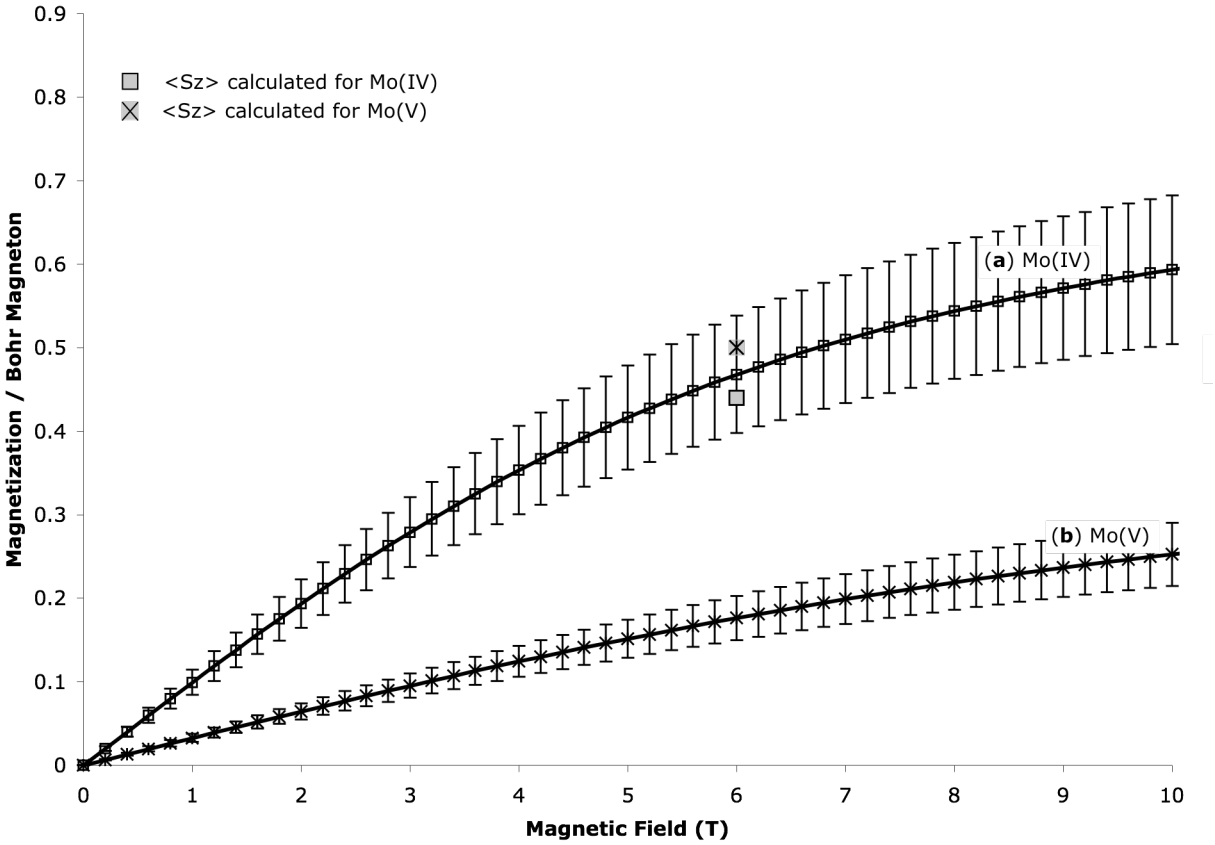

Figure 4. Theoretical spin magnetization per Mo ion along with the experimental values measured at H = 6 T. Curve **a** and the shadowed square are for Mo(IV) and curve **b** and the shadowed cross are for Mo(V).

In order to confirm the absence of charge transfer, we measured the XAS spectra at the Cu K-edge (Fig. 3). In the CsMoCu compound, there are two sites for Cu ions: Cu^{II} ions with a square based pyramidal geometry, linked with five Mo(CN) units, and Cu^{II} ions in a square planar configuration [44]. XANES spectra allow the investigation of the valence and the local geometry of atoms. According to the literature, Cu^{I} ions are characterized by a pre-edge around 8980-8983 eV, whereas Cu^{II} ions display a pre-edge at 8986-8989 eV [52-57]. The edge peak, corresponding to peak B in Fig.3 is located 13 eV higher than the pre-edge peak A. In Fig.3 peak A (8987.1 eV) on spectrum **1** (that is before illumination) is then consistent with Cu^{II} ions. With photoillumination, one observes only small modifications of the copper pre-edge. Peak A intensity increases by 2%

of the atomic absorption with no noticeable energy shift. Moreover spectra **2** and **3** in Fig. 3 are almost identical so that there is no spectroscopic evidence that Cu ions are involved in the thermally induced relaxation. The small difference between spectra **1** and **2** (2% at peak A, and 5 % at peak B) are likely to come from some degradation of the sample under the laser illumination. Then Cu ions are not involved in the photo-induced magnetism in the compound.

Conclusion

We have measured the photomagnetic properties of nanoparticles of the extended network $Cs_{0,5}Cu_{1,75}[Mo(CN)_8]$ by SQUID magnetometry and XMCD at Mo $L_{2,3}$ edges and we have also recorded the XAS spectra at the Cu K edge after irradiation. The charge transfer hypothesis is not compatible with the present measurements and the only way to interpret them is to suppose the existence of a photoinduced LS Mo(IV) to HS Mo(IV) transformation. Within this hypothesis, the large increase of the magnetization per formula unit is explained by the fact that the magnetization at saturation of the molecular unit $Cs_{0.5}Cu_{1,75}[Mo(CN)_8]$ is 1.75 μ_B before photoexcitation and 3.75 μ_B after photoexcitation. The average magnetic moment of Mo ions measured by XMCD ($\approx$ 0.42 μB) corresponds to a 35 % ± 5 % photoconversion of LS Mo(IV) ions into HS Mo(IV) ions. The absence of signature for the presence of Cu(I) ion at Cu K-edge and also the absence of any reversible change at the Cu K edge clearly indicate that copper ions are not involved in the photoconversion.

Acknowledgements

We acknowledge the help from Giordano Poneti and Matteo Mannini who kindly provided us with their whole 405 nm laser set-up which made the experiment possible. We thank the CNRS (Centre National de la Recherche Scientifique), the French programme ANR-blanc (project MS-MCNP), and the European community for financial support (contract NMP3-CT-2005-515767 NoE “MAGMANET”) for financial support.

References

(1) Bonhommeau, S.; Molnar, G.; Galet, A.; Zwick, A.; Real, J. A.; McGarvey, J. J.; Bousseksou, A. *Angewandte Chemie International Edition* **2005**, *44*.

(2) Entley, W. R.; Girolami, G. S. *Science* **1995**, *268*, 397.

(3) Ferlay, S.; Mallah, T.; Ouahès, R.; Veillet, P.; Verdaguer, M. *Nature* **1995**, *378*, 701.

(4) Niel, V.; Martinez-Agudo, J. M.; Munoz, M. C.; Gaspar, A. B.; Real, J. A. *Inorganic Chemistry* **2001**, *40*, 3838.

(5) Sato, O.; Iyoda, T.; Fujishima, A.; Hashimoto, K. *Science* **1996**, *272*, 704.

(6) Verdaguer, M.; Bleuzen, A.; Marvaud, V.; Vaissermann, J.; Seuleiman, M.; Desplanches, C.; Scuiller, A.; Train, C.; Garde, R.; Gelly, G.; Lomenech, C.; Rosenman, L.; Veillet, P.; Cartier dit Moulin, C.; Villain, F. *Coordination Chemistry Reviews* **1999**, *190-192*, 1023.

(7) Boldog, I.; Gaspar, A. B.; Martinez, V.; Pardo-Ibanez, P.; Ksenofontov, V.; Bhattacharjee, A.; Gütlich, P.; Real, J. A. *Angewandte Chemie International Edition* **2008**, *47*, 6433.

(8) Brinzei, D.; Catala, L.; Mathonière, C.; Wernsdorfer, W.; Gloter, A.; Stephan, O.; Mallah, T. *Journal of the American Chemical Society* **2007**, *129*, 3778.

(9) Catala, L.; Gacoin, T.; Boilot, J.-P.; Rivière, E.; Paulsen, C.; Lhotel, E.; Mallah, T. *Advanced Materials* **2003**, *15*, 826.

(10) Catala, L.; Mathonière, C.; Gloter, A.; Stephan, O.; Gacoin, T.; Boilot, J.-P.; Mallah, T. *Chemical Communications* **2005**, 746.

(11) Catala, L.; Volatron, F.; Brinzei, D.; Mallah, T. *Inorganic Chemistry* **2009**, *48*, 3360.

(12) Clavel, G.; Larionova, J.; Guari, Y.; Guérin, C. *Chemistry A European Journal* **2006**, *12*, 3798.

(13) Frye, F. A.; Pajerowski, D. M.; Anderson, N. E.; Long, J.; Park, J. H.; Meisel, M. W.; Talham, D. R. *Polyhedron* **2007**, *26*, 2273.

(14) Larionova, J.; Salmon, L.; Guary, Y.; Tokarev, A.; Molvinger, K.; Molnar, G.; Bousseksou, A. *Angewandte Chemie International Edition* **2008**, *47*, 8236.

(15) Moore, J. G.; Lochner, E. J.; Ramsey, C.; Dalal, N. S.; Stiegma, A. E. *Angewandte Chemie International Edition* **2003**, *42*, 2741.

(16) Clavel, G.; Guari, Y.; Larionova, J.; Guerin, C. *New Journal of Chemistry* **2005**, *29*, 275.

(17) Ferlay, S.; Mallah, T.; Ouahes, R.; Veillet, P.; Verdaguer, M. *Inorganic Chemistry* **1999**, *38*, 229.

(18) Bleuzen, A.; Marvaud, V.; Mathonière, C.; Sieklucka, B.; Verdaguer, M. *Inorganic Chemistry* **2009**, *48*, 3453.

(19) Sato, O. *Journal of Photochemistry and Photobiology C: Photochemistry Reviews* **2004**, *5*, 203.

(20) Escax, V.; Champion, G.; Arrio, M.-A.; Zacchigna, M.; Cartier dit Moulin, C.; Bleuzen, A. *Angewandte Chemie* **2005**, *44*, 1798.

(21) Yokoyama, T.; Ohta, T.; Sato, O.; Hashimoto, K. *Physical Review B* **1998**, *58*, 8257.

(22) Yokoyama, T.; Kigushi, M.; Ohta, T.; Sato, O.; Einaga, Y.; Hashimoto, K. *Physical Review B* **1999**, *60*, 9340.

(23) Ohkoshi, S.-i.; Hashimoto, K. *Journal of Photochemistry and Photobiology C: Photochemistry Reviews* **2001**, *2*, 71.

(24) Cartier dit Moulin, C.; Villain, F.; Bleuzen, A.; Arrio, M.-A.; Sainctavit, P.; Lomenech, C.; Escax, V.; Baudelet, F.; Dartyge, E.; Gallet, J.-J.; Verdaguer, M. *Journal of the American Chemical Society* **2000**, *122*, 6653.

(25) Shirom, M.; Weiss, M. *Journal of Chemical Physics* **1972**, *56*, 3170.

(26) Champion, G.; Escax, V.; Cartier dit Moulin, C.; Bleuzen, A.; Villain, F.; Baudelet, F.; Dartyge, E.; Verdaguer, M. *Journal of the American Chemical Society* **2001**, *123*, 12544.

(27) Herrera, J. M.; Bachschmidt, A.; Villain, F.; Bleuzen, A.; Marvaud, V.; Wernsdorfer, W.; Verdaguer, M. *Philosophical Transactions of the Royal Society A* **2008**, *366*, 127.

(28) Shirom, M.; Siderer, Y. *Journal of Chemical Physics* **1973**, *58*, 1250.

(29) Hennig, H.; Rehorek, A.; Rehorek, D.; Thomas, P. *Inorganica Chimica Acta* **1984**, *86*, 41.

(30) Hennig, H.; Rehorek, A.; Rehorek, D.; Thomas, P.; Bäzold, D. *Inorganica Chimica Acta* **1983**, *77*, L11.

(31) Herrera, J. M.; Marvaud, V.; Verdaguer, M.; Marrot, J.; Kalisz, M.; Mathonière, C. *Angewandte Chemie* **2004**, *116*, 5584.

(32) Ma, X.-D.; Yokoyama, T.; Hozumi, T.; Hashimoto, K.; Ohkohi, S.-i. *Physical Review B* **2005**, *72*, 094107.

(33) Rehorek, D.; Salvetter, J.; Hantschmann, A.; Hennig, H.; Stasicka, Z.; Chodkowska, A. *Inorganica Chimica Acta* **1979**, *37*, L471.

(34) Ohkoshi, S.-i.; Machida, N.; Zhong, Z. J.; Hashimoto, K. *Synthetic Metals* **2001**, *122*, 523.

(35) Mathonière, C.; Kobayashi, H.; Le Bris, R.; Kaïba, A.; Bord, I. *C. R. Chimie* **2008**, *11*, 665.

(36) Rombaut, G.; Verelst, M.; Golhen, S.; Ouahab, L.; Mathonière, C.; Kahn, O. *Inorganic Chemistry* **2001**, *40*, 1151.

(37) Rombaut, G.; Mathonière, C.; Guionneau, P.; Golhen, S.; Ouahab, L.; Verelst, M.; Lecante, P. *Inorganica Chimica Acta* **2001**, *326*, 27.

(38) Arrio, M.-A.; Long, J.; Cartier dit Moulin, C.; Bachschmidt, A.; Marvaud, V.; Rogalev, A.; Mathonière, C.; Wilhelm, F.; Sainctavit, P. *Journal of Physical Chemistry C* **2010**, *114*, 595.

(39) Christou, G.; Gatteschi, D.; Hendrickson, D. N.; Sessoli, R. *MRS Bulletin* **2000**, 66.

(40) Gatteschi, D. *Journal of Alloys and Compounds* **2001**, *317-318*, 8.

(41) Carra, P.; Thole, B. T.; Altarelli, M.; Wang, X. *Physical Review Letters* **1993**, *70*, 694.

(42) Thole, B. T.; Carra, P.; Sette, F.; van der Laan, G. *Physical Review Letters* **1992**, *68*, 1943.

(43) Carjaval, M.-A.; Reguero, M.; De Graaf, C. *Chemical Communications* **2010**, *46*, 5737.

(44) Hozumi, T.; Hashimoto, K.; Ohkohi, S.-i. *Journal of the American Chemical Society* **2005**, *127*, 3864.

(45) Volatron, F.; Catala, L.; Rivière, E.; Gloter, A.; Stephan, O.; Mallah, T. *Inorganic Chemistry* **2008**, *47*, 6584.
(46) Volatron, F., Université Paris XI, 2010.
(47) Volatron, F.; Heurtaux, D.; Catala, L.; Mathonière, C.; Clemente-Léon, M.; Lopez, A.; Coronado, E.; Repetto, D.; Gloter, A.; Mallah, T. **2010** *(To be published)*.
(48) Ohkoshi, S.-i.; Tokoro, H.; Hozumi, T.; Zhang, Y.; Hashimoto, K.; Mathonière, C.; Bord, I.; Rombaut, G.; Verelst, M.; Cartier dit Moulin, C.; Villain, F. *Journal of the American Chemical Society* **2006**, *128*, 270.
(49) Facility, E. S. R.
(50) Lefebvre, D.; Sainctavit, P.; Malgrange, C. *Review of Scientific Instruments* **1994**, *65*, 2556.
(51) Thole, B. T.; van der Laan, G. *Physical Review A* **1988**, *38*, 38.
(52) Kurisaki, T.; Matsuo, S.; Yamashige, H.; Wakita, H. *Journal of Molecular Liquids* **2005**, *119*, 153.
(53) Studer, F.; Bourgault, D.; Martin, C.; Retoux, R.; Michel, C.; Raveau, B.; Dartyge, E.; Fontaine, A. *Physica C* **1989**, *159*, 609.
(54) Soderholm, J.; Goodman, G. L. *Journal of the Optical Society of America B* **1989**, *6*, 483.
(55) Kau, L.-S.; Spira-Solomon, D. J.; Penner-Hahn, J. E.; Hodgson, K. O.; Solomon, E. I. *Journal of the American Chemical Society* **1987**, *109*, 6433.
(56) Benzekri, A.; Cartier, C.; Latour, J.-M.; Limosin, D.; Rey, P.; Verdaguer, M. *Inorganica Chimica Acta* **1996**, *252*, 413.
(57) Irie, H.; Kamiya, K.; Shibanuma, T.; Miura, S.; Tryk, D. A.; Yokoyama, T.; Hashimoto, K. *Journal of Physical Chemistry C* **2009**, *113*, 10761.

Supplementary Information

Investigation of the photoinduced magnetization of Copper octacyanomolybdates nanoparticles by X-ray Magnetic Circular Dichroism. *by Sophie Brossard et al.*

A-Magnetic measurements.

Experimental section :

Photomagnetic experiments were carried out with two Quantum Design magnetometer (one MPMS-XL and one MPMS-XL) in the dc mode. The measurements were performed in the 2-300K range with magnetic field of 100 G, and at 2 K, 5 K and 9 K up to 7 Teslas for magnetizations. The photomagnetic experiments were performed with a Ar^{+}-Kr^{+} laser coupled through an optical fiber directed into the squid cavity. The output of the fiber is situated to a distance of 4 cm. Coated nanoparticules were laid down on the sample holder. The diamagnetic contribution and the weight were estimated by comparing the magnetization vs. magnetic field at 5 K and χ curves measured in the 2-300K before irradiation with those recorded for the sample in a routine experiment (6,50 mg of sample loaded into a polymer bag).

During irradiation, performed at 10 K under 100 Oe, the magnetic susceptibility is increasing, and after 22 hours, starts to saturate (Fig.SIa). After irradiation, the opening of the hysteresis loop (Fig.S1b) clearly indicates the magnet-like behaviour of the metastable photomagnetic phase.

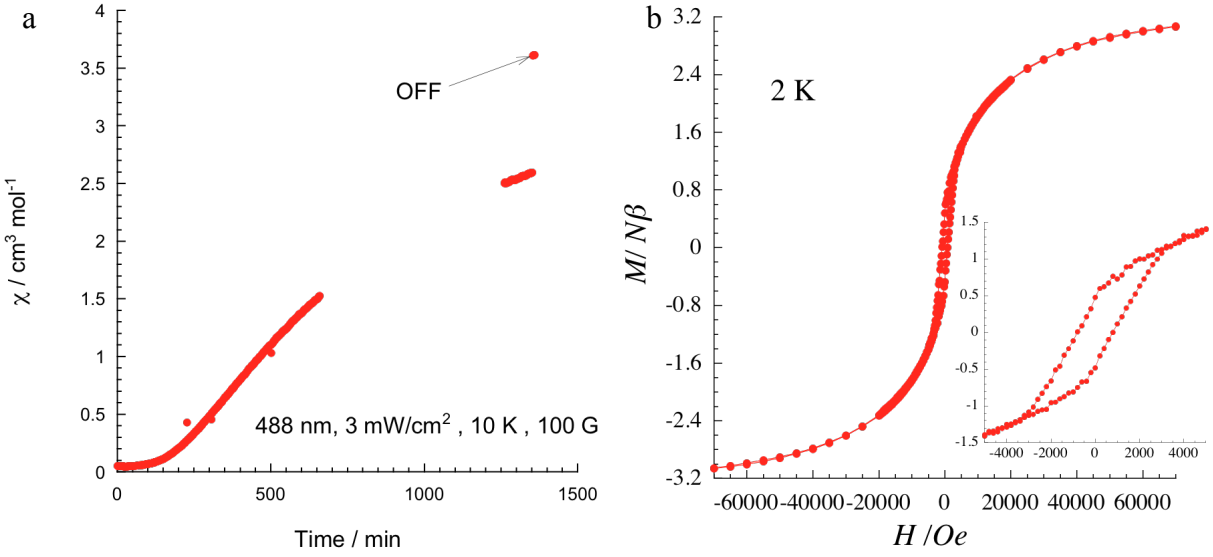

Figure S1. (a) Magnetic susceptibility measured at H = 100 Oe before and after illumination of the compound; (b) M=f(H) measured at 2 K after irradiation [46,47]

B-Normalization procedure.

For normalization, one calculate the integral of the continuum states i.e. from 2533.1 eV to 2555.7 eV for the Mo L_3 edge, from 2637.6 to 2663.2 eV for Mo L_2 and from 9012.3 to 9041.2 eV for Cu K edge. Then the spectra are divided by the continuum integral. One then normalizes the L_3 edge jump to 2, the L_2 edge jump to 1 and the copper edge jump to 1. Doing so, normalization is independent of the continuum oscillations since it is not performed on one single arbitrary point. In a next step, conventional fluorescence corrections are applied to account for the non linearity between the measured Total Fluorescence Yield and the cross sections.

C-X-ray induced radiation damage.

Figure S2 and S3 indicate the spectral modifications induced by x-ray radiation damage. After XMCD measurements, relaxation is less complete than it is observed in Fig.1 where x-ray damages have been minimized.

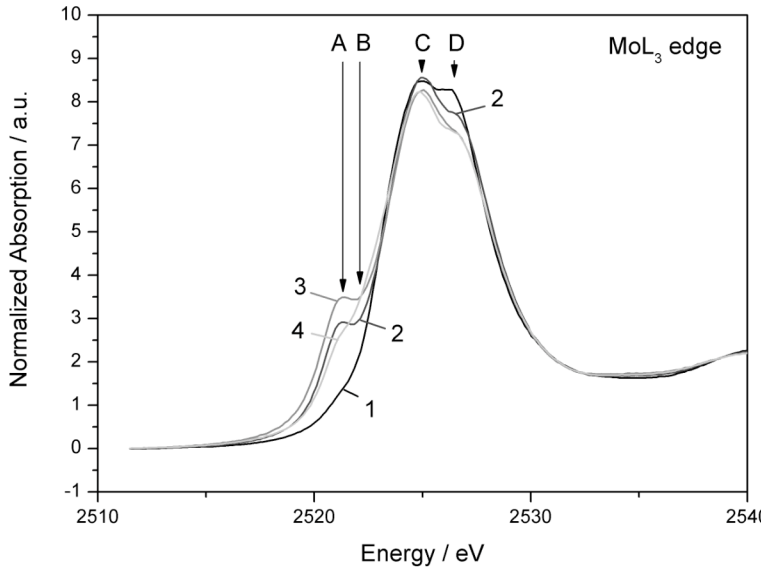

Figure S2. Absorption spectra at the Mo L_3 edge (**1**) before illumination (T = 9K), (**2**) after illumination (T = 9K), (**3**) after X-ray irradiation consecutive to XMCD measurements (T = 9K) and (**4**) after relaxation at room temperature (T = 300K).

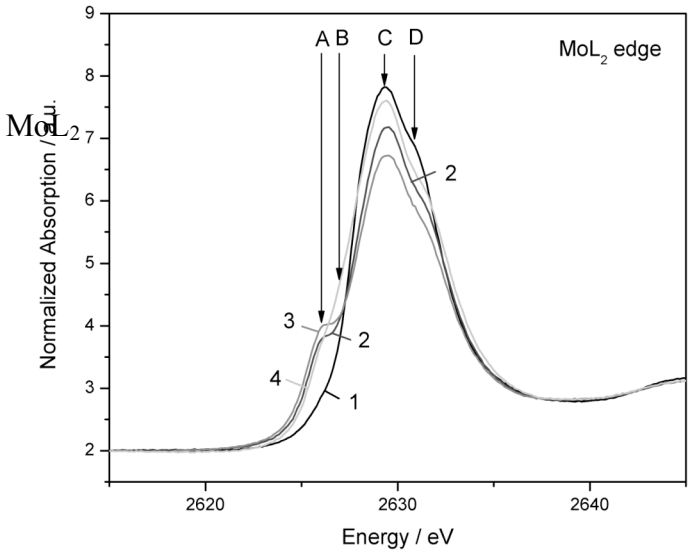

Figure S3. Absorption spectra at the Mo L_2 edge (**1**) before illumination (T = 9 K), (**2**) after illumination (T = 9 K), (**3**) after X-ray irradiation consecutive to XMCD measurements (T = 9 K) and (**4**) after relaxation at room temperature (T = 300 K).

D- Yield of photoconversion.

The yield of photoconversion can be estimated by comparison of the Mo L_3 edge spectra of the photoconverted phase from Ref.[38] and Ref.[27]. Figure S4 reports spectra 1 and 2 of Fig.1 and the difference signal between the two spectra. Figure S5 reports the spectra before irradiation and after x-ray induced irradiation of the photomagnetic molecule $[Mo(CN)_6(CN\text{-}CuL'_2)_2]$ (L' = *N, N'* dimethyl ethylene diamine) from Ref.[38] where the rate of photoconversion could be estimated to 100%. By comparison of the difference signals from Figures S4 and S5, the yield of

Figure S4. Mo L_3 edge spectra 1 and 2 of Figure 1 and the associated difference.

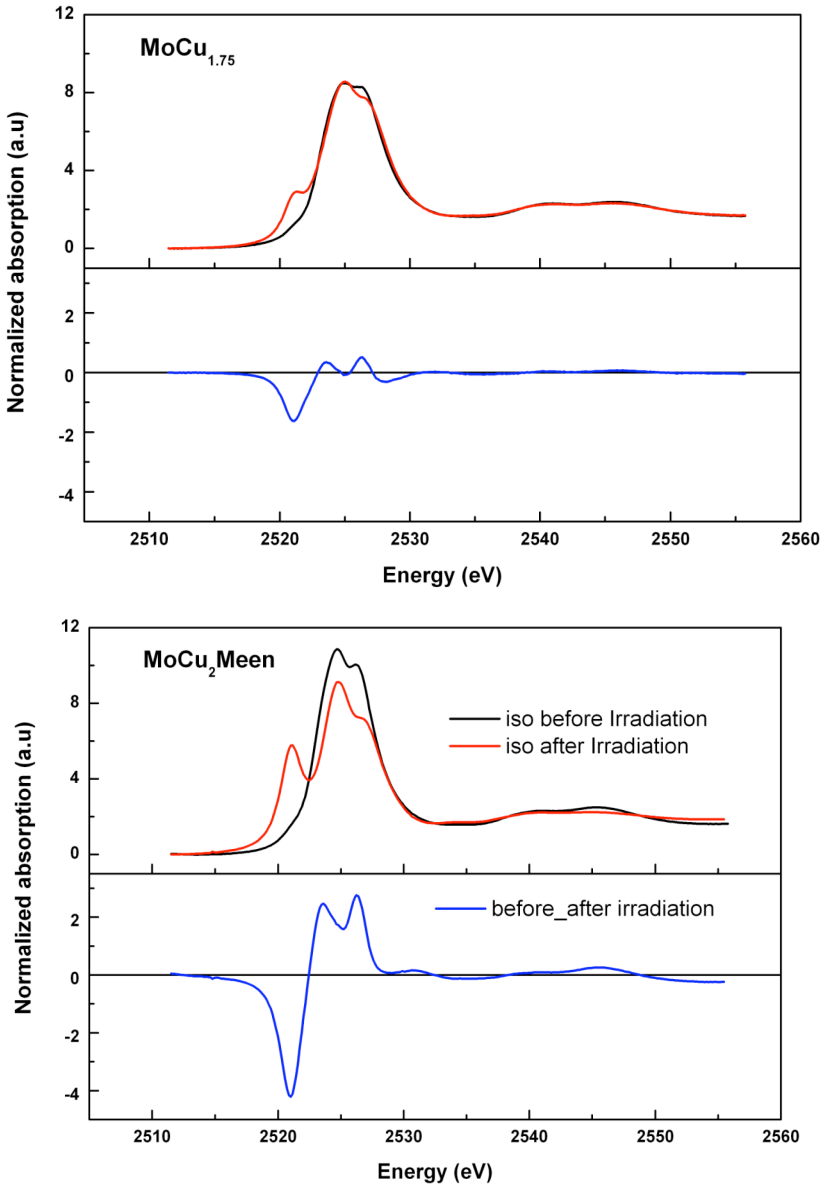

the figures have not exactly the same size which render the peak-to-peak analysis more dofficult. Please resize the two figures

Figure S5. Mo L_3 edge spectra at 10 K before and after x-ray irradiation of the photomagnetic molecule $[Mo(CN)_2(CN\text{-}CuL)_6]^{8+}$ from Ref.[38] and the associated difference.

photoconversion in the present study can be estimated to be 30%. A similar comparison can be performed with the spectra measured by Herrera *et al.* [27] and this would give a photoconversion rate of 40%. We then conclude that the actual photoconversion rate for the present study is 35 % ± 5%.

E-Magnetization curve

Figure S6 reports figure 4 of the paper plus curve **c** that is the expected magnetic moment deduced from the experimental magnetization curve for the photomagnetic phase. Curve **c** is the same as curve in Fig.1b multiplied by 35% to account for incomplete photoconversion and multiplied by 2/3.75 assuming that Mo ions contributes for 2 Bohr magnetons for a magnetization at saturation of 3.75 Bohr magnetons/f.u (this analysis supposes that the 100% photoconversion for the SQUID measurements have been obtained. However, the maximum value of the saturation is 3.1 NB suggesting that you have a photoconversion 80 % with the SQUID measurements. Applying the ratio, I think that we get almost the experimental value). From Fig.S6, it is clear that curve **c** is consistent with the existence Low Spin to High Spin conversion scheme. No such curve can be plotted in the hypothesis of a Mo to Cu charge transfer since the measured magnetization per f.u. is much larger that the expected magnetization at saturation for the charge transfer model.

Figure S6. Same as figure 4 plus curve **c** giving the Mo magnetizaton as extracted from the experimental SQUID measurements.